

**Research Article****INFLUENCE OF SOLVENT ON STRUCTURAL, MORPHOLOGICAL AND OPTICAL PROPERTIES OF  $\text{SnO}_2$  NANOPARTICLES PREPARED BY DIFFERENT METHODS****Backialakshmi P and Gopinathan C\***

Department of Solar Energy, School of Energy, Environment and Natural Resources, Sciences, Madurai Kamaraj University, Madurai - 625 021, Tamil Nadu, India

DOI: <http://dx.doi.org/10.24327/ijrsr.2017.0809.0761>**ARTICLE INFO****Article History:**Received 18<sup>th</sup> June, 2017Received in revised form 10<sup>th</sup> July, 2017Accepted 06<sup>th</sup> August, 2017Published online 28<sup>th</sup> September, 2017**Key Words:**

Tin oxide, Co-precipitation, Sol-gel, XRD, optical properties

**ABSTRACT**

This study represents comparisons between the structural, morphologies and optical properties of tin oxide ( $\text{SnO}_2$ ) nanoparticles prepared by two different methods, namely the Sol-gel and the Co-precipitation methods. The characteristics of the particles were analyzed using X-ray diffraction (XRD), Fourier transform infrared spectroscopy (FTIR), Scanning electron microscopy (SEM) and Energy Dispersive X ray spectroscopy (EDS). The optical properties were analyzed using UV-vis spectroscopy (UV-vis). Using XRD study recognized the structure of a single phase of  $\text{SnO}_2$  nanoparticles of both methods. It has been enormous that solvents played main role in varying the crystallite size of tin oxide nanoparticles in Sol-gel and Co-precipitation methods. From two different types of method, the crystallite size of  $\text{SnO}_2$  nanoparticles varies mutually solvent and method. Using the two-different method XRD study showed well crystallized tetragonal  $\text{SnO}_2$  can be obtained and the crystal sizes were 16.71, 5.43 and 10.09 nm for the sample of water, methanol and ethanol. In Co-precipitation method the crystal sizes were 18.71, 9.9 and 11.7 nm for the sample of water, methanol and ethanol. In sol-gel method and Co-precipitation X-Ray Diffraction (XRD) patterns showed extremely crystalline single phase tetragonal structure, with a main (110) plane in water and methanol samples and (101) for ethanol samples in the method I. In the Co-precipitation method, with predominant (101) plane in methanol and ethanol sampled and (110) for water samples. With the above analysis, we will discuss that the Co-precipitation may be appreciated for time consuming and high yield of particles.

**Copyright © Backialakshmi P and Gopinathan C, 2017**, this is an open-access article distributed under the terms of the Creative Commons Attribution License, which permits unrestricted use, distribution and reproduction in any medium, provided the original work is properly cited.

**INTRODUCTION**

Tin oxide is a capable efficient material owing to its properties such as strong physical and chemical interaction with adsorbed species, low operating temperature and high degree of transparency in the visible region (Adnan *et al.*, 2010; Zhu *et al.*, 2006). Tin oxide ( $\text{SnO}_2$ ) is an n-type broad band semiconductor ( $E_g = 3.6$  eV at 300 K) and generally used as an foremost functional material for catalyst support and gas sensing material, optoelectronic devices, transparent conductive electrodes, solar cells, (Peaker and Horsley (1971); Drevillon *et al.*, 1989). In the interior the wide family of efficient materials, metal oxides are particularly attractive owing to their applications in sensing, catalysis, energy storage and conversion, optics and electronics (Niederberger, (2007)). Titanium oxide ( $\text{TiO}_2$ ), Zinc oxide ( $\text{ZnO}$ ), and Tin oxide ( $\text{SnO}_2$ ) is the centre of exact interest due to their only structural, optical, and catalytic properties (Vij *et al.*, 2012; Das

and Jayaraman (2014); Wang *et al.*, 2015). Above all, the attention in  $\text{SnO}_2$  has increased due to its properties like high transparency, little electrical sheet resistance and high chemical strength (Minami, (2000); Young *et al.*, 2002). In addition  $\text{SnO}_2$  is also of huge methodical and technological notice due to its multitalented applications in dye-based solar cells, gas sensors, optical devices and electronic devices transparent conducting electrodes etc. (Hieu *et al.*, 2012; Park *et al.*, 2013; Deng and Lee (2008)). Owing to the modifications in properties of nanomaterials, in recent times the mind has been unfocused to synthesize and characterize  $\text{SnO}_2$  nanoparticles by dissimilar methods. The applications and properties of nanostructured materials are partial intensely by their size, structure, morphology, and chemical composition. Still the achievement in a lot of of these applications relies on the capability in obtaining cost effective, high eminence nano sized materials having standardized grain structures (Henglein, (1989); Alivisatos, (1996); Burda *et al.*, 2005). It is fine known that the

\*Corresponding author: Gopinathan C

Department of Solar Energy, School of Energy, Environment and Natural Resources, Sciences, Madurai Kamaraj University, Madurai - 625 021, Tamil Nadu, India

helpful presentation of SnO<sub>2</sub> is qualified to its, morphology, crystal size, surface properties crystal defects and crystallinity etc. which eventually depends on the investigate methods and preparation situation (Leite *et al.*, 2000; Jiang *et al.*, 2005). Throughout nanoparticle research, solvent plays a very essential role in a reaction mechanism. Solvent provides a means of temperature control by determining the highest temperature at which reaction will arise (Ungula and Dejene (2015). Before studies also indicated that particle growth and coarsening are powerfully reliant on solvent through the, surface energy, bulk solubility and viscosity (Hu *et al.*, 2003). Thus by through dissimilar solvents the control over SnO<sub>2</sub> nanoparticles size and size division could be achieved, which is essential for optical, tailoring, electrical, magnetic and chemical and properties of nanoparticles for exact applications. SnO<sub>2</sub> is an interesting metal oxide because it can exist in diverse convoluted morphologies (Guan *et al.*, 2013). SnO<sub>2</sub> has been syntheses by diverse methods such as, hydrothermal methods (Huang *et al.*, 2001), solid state synthesis (Gautam *et al.*, 2013), chemical vapor deposition (Kennedy *et al.*, 2003), colloidal and aerosol routes (Zhang *et al.*, 2012) co-precipitation (Nomura *et al.*, 2011) and sol-gel method (Kumar *et al.*, 2016). In dissimilarity to high temperature production, co-precipitation is one of the favored methods and has recompense such as the option of obtaining metastable materials, achieving better purity and compositional homogeneity of the products at restrained temperatures and the necessity of easy laboratory equipments (Niederberger, (2007). In this, the influences of solvent on the structural, morphological, and optical properties of SnO<sub>2</sub> nanoparticles using two different methods have been reported. In this study, ethanol, methanol, water were used as solvent media. The polar characteristic of solvent was the major factor that affects both growth and nucleation and of SnO<sub>2</sub> nanoparticles, and, as a result, determines the size, shape, and piece ratio of the product (Ungula and Dejene, (2015). Therefore, the mainly significant of this examine paper was to learn the influence of solvent on the structural, morphology, size, and optical properties of synthesized nanoparticles using sol-gel and Co-precipitation method.

## MATERIALS AND METHODS

### Experimental

All chemical reagents were marketable with AR purity, and used directly without further purification.

### Sol-gel method

Two different types of SnO<sub>2</sub> particles were prepared using common Co-precipitation (Nomura *et al.*, 2011) and sol-gel (Kumar *et al.*, 2016). In a Sol-gel method, SnO<sub>2</sub> nanostructures was prepared by dissolving 0.5 g of SnCl<sub>2</sub>.2H<sub>2</sub>O was dissolved in 100 ml Methanol. The resulted precursor combination was reserved for stirring on a magnetic stirrer and while stirring into this mixture for 30 minutes. The aqueous ammonia solution was added in drop wise manner (with a rate of 5 drops/minute). On adding of approximately 40-50 drops of aqueous ammonia the sol-gel was produced around within the 15 minutes. The resultant opal gels were washed with ethanol to remove impurities, and dried over 80 °C for 5 h in order to remove water molecules. Finally, ash colored tin oxide nanopowders

were formed at 400 °C for 2 h. The same procedure was followed for the preparation of tin oxide nanoparticles using ethanol and water as a solvent.

### Co-precipitation Method

In Co-precipitation method, SnO<sub>2</sub> nanoparticles was prepared by dissolving 1g stannous chloride dehydrates in 100 ml distilled water. After complete finish, 4ml ammonia solution was added drop wise to the above solution by under stirring. The solution was further stirred for 2 h, and then a few drops of H<sub>2</sub>O<sub>2</sub> were added while stirring until the solution changed color. The result was then washed and filtered two times, dried in an oven at 150 °C for 4 h, and calcined at 500 °C for 2 h. In the present study, the calcinations temperature used was 500 °C because the alteration of SnO to SnO<sub>2</sub> occurs at 500-600 °C by direct heating (Allaedini *et al.*, 2015). The same procedure was followed for the preparation of tin oxide nanoparticles using ethanol and Methanol as a solvent.

## RESULTS AND DISCUSSION

### XRD

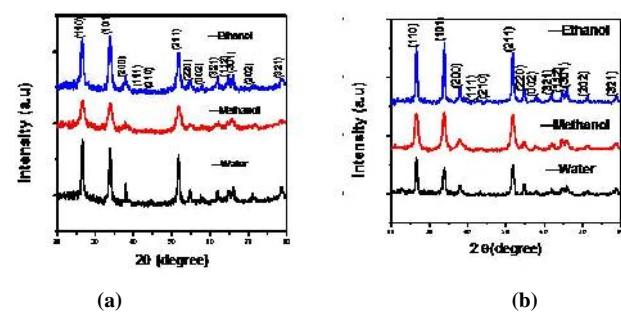


Fig 1(a), (b) XRD patterns of the synthesized SnO<sub>2</sub> using: (a) Sol-gel method, (b) Co-precipitation method

Table 1 Sol-Gel method

Sample	d spacing(hkl)	Crystallite Size (nm)	Lattice parameters			
			Calculated a(Å)	Standard a(Å)	Calculated c(Å)	Standard c(Å)
Synthesis in Water	3.3394 (110)	16.71	4.7226	4.7370	3.1718	3.1850
Synthesis in Methanol	3.3467 (110)	5.43	4.7245	4.7370	3.1704	3.1850
Synthesis in Ethanol	2.6469 (101)	10.09	4.7591	4.7370	3.1917	3.1850

Table 2 Chemical Co-precipitation method

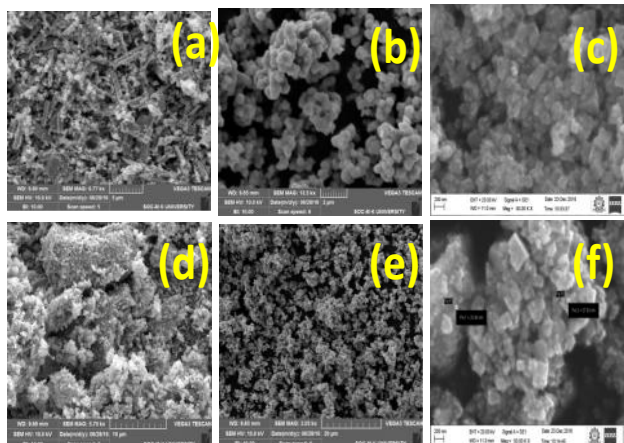
Sample	d spacing (hkl)	Crystallite Size (nm)	Lattice parameters			
			Calculated a(Å)	Standard a(Å)	Calculated c(Å)	Standard c(Å)
Synthesis in Water	3.3484 (110)	18.9	4.7354	4.7370	3.1622	3.1850
Synthesis in Methanol	2.6467 (101)	9.9	4.7582	4.7370	3.1914	3.1850
Synthesis in Ethanol	2.6474 (101)	11.7	4.7620	4.7370	3.1925	3.1850

Fig. 1(a) (b) shows the XRD patterns of the prepared SnO<sub>2</sub> nanoparticles using two methods at various solvents (water, methanol, ethanol respectively). All diffraction peaks can be readily indexed to tetragonal SnO<sub>2</sub> phase (JCPDS card No.72-1147). No other peaks were observed such as Sn or any other Sn based oxide, which represents the superior purity of the samples. The diffraction peaks are noticeably broadened, which indicates that the crystalline sizes of samples are extremely tiny. The sharpness and peak intensity increases responds on

solvents, which reveals that the grain sizes become larger and the crystallinity improved. According to the Debye-Scherer's equation, the crystallite sizes was calculated to be 16.71, 5.43 and 10.09 nm for the samples prepared with water, methanol, ethanol for Co-precipitation method and it was 18.9, 9.9 and 11.7 nm for the samples prepared at various solvents for sol-gel method, respectively). No diffraction peaks due to metallic Sn or other impurities were observed, indicating the single-phase formation of the nanoparticles. In the tetragonal structure of  $\text{SnO}_2$  lattice parameters ( $a = b$ , and  $c$ ) have been calculated from the XRD peaks using the equation [27]:

### Sem

The SEM image of synthesized  $\text{SnO}_2$  nanoparticles using a sol-gel method with different solvents were shown in Fig 2 (a-c), which indicates that  $\text{SnO}_2$  nanoparticles have different morphologies with different solvents such as water, methanol and ethanol respectively. Fig 2 (a) shows that the  $\text{SnO}_2$  nanoparticles have rod like morphology. Also, the rods are highly agglomerated with uniform distribution. Fig. 2 (b) shows that most of the  $\text{SnO}_2$  nanoparticles have a spherical shape. Here, several particles are combined themselves, which is looking like group of atoms are formed as a molecule. Also, the segregations among the groups of spherical shape nanoparticles. Fig 2(c) shows that the morphology of  $\text{SnO}_2$  nanoparticles has a square



**Fig 3 (a-c)** shows the SEM images of Sol-gel and (d-f) shows the SEM images of Co-precipitation method

Shape which spreads uniformly throughout the image. Here, the square shaped nanoparticles are highly agglomerated than rod like morphology. The SEM image of synthesized  $\text{SnO}_2$  nanoparticles using a Co-precipitation method with different solvents was shown in Fig 2 (d-f), which indicates that  $\text{SnO}_2$  nanoparticles have different morphologies with different solvents such as water, methanol and ethanol respectively. Fig 2(d) shows that the morphology of  $\text{SnO}_2$  nanoparticles has cluster-like formation. Fig 2 (e) shows that most of the  $\text{SnO}_2$  nanoparticles have a spherical shape. Fig. 2 (f) shows that the morphology of  $\text{SnO}_2$  nanoparticles has a square shape which spreads uniformly throughout the image. The occurrence of chemical elements Sn, O, and Cu can be observed in this graph. The atomic weight percentage is shown in Table 3. It is clear from Table 3 that oxygen has a comparatively large atomic weight percentage showing that  $\text{SnO}_2$  was attained. On the other hand, some traces of carbon element were too found,

which could be credited to the carbon tape of the sample holder.

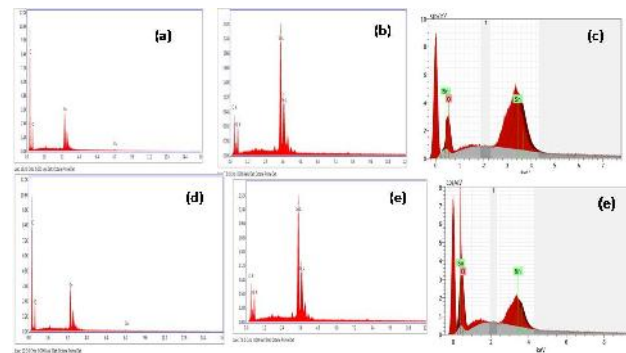


**Fig 3 (a-c)** shows the EDX graphs for both the sol-gel (d-e) Co-precipitation methods.

**Table 3** Atomic weight percentage result obtained by EDX

Sample	Method	Weight %	Atomic %
Sn	Sol-gel	55.56	27.00
O	Sol-gel	28.05	0.88
C	Sol-gel	17.31	70.86
Sn	Co-precipitation	50.87	22.85
O	Co-precipitation	36.62	0.68
C	Co-precipitation	22.63	65.36

### FTIR

The FTIR spectra of tin oxide powder synthesized by the Sol-gel and the Co-precipitation. Methods using different solvents such as water, methanol and ethanol within 400-4000  $\text{cm}^{-1}$  are shown in Fig. 4(a, b). For pure  $\text{SnO}_2$ , the different absorption bands to be found at 672, 1,022, 1,627, 2,926, 3,395  $\text{cm}^{-1}$  are observed. Broad absorption bands centered at 673 and 1021  $\text{cm}^{-1}$  can be assigned to the stretching vibrations of Sn-O and bending vibrations of O-Sn-O bonds, respectively. From Fig. 4 it is observed that the position of Sn-O is centered at 673, 621, and 619  $\text{cm}^{-1}$ , for water, methanol, ethanol respectively, for co-precipitation route and centered at 617, 655 and 612  $\text{cm}^{-1}$ , for water, methanol, and ethanol respectively for sol-gel method.

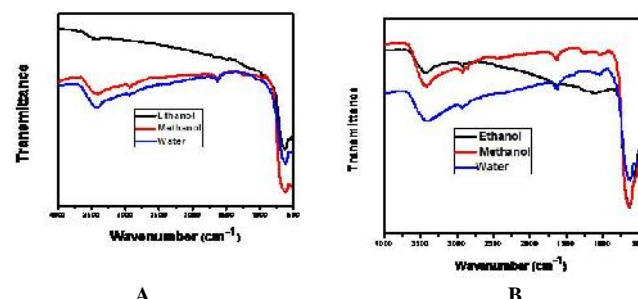


**Fig 4 (a, b)** shows the FTIR spectrum of  $\text{SnO}_2$  nanoparticles prepared in different solvents using Sol-gel and Co-precipitation method.

UV-vis absorption spectra of  $\text{SnO}_2$  nanoparticles prepared by different solvents using sol-gel method and Co-precipitation method. Fig. 5 (a, b) shows the UV-vis absorption spectra of  $\text{SnO}_2$  nanoparticles synthesized by different solvents sol-gel method, Co-precipitation method. In sol-gel method the band gap is established to be 3.67 eV, 3.63 eV, 3.57 eV equivalent to nanoparticles synthesized by different solvent (water, methanol, ethanol), respectively.

### UV-visible Analysis

In the Co-precipitation method, the band gap is established to be 3.62 eV, 3.59 eV, 3.52 eV synthesized by different solvent (water, methanol, ethanol), respectively.

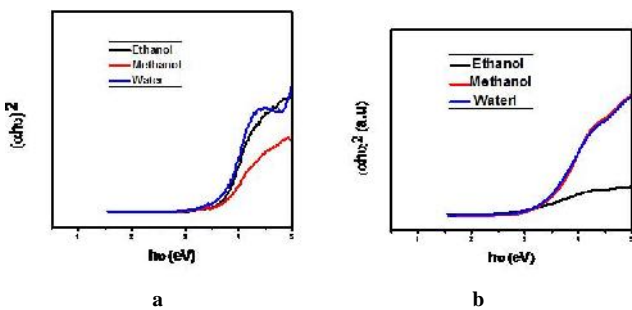


**Fig 5 (a, b)** shows the UV-vis Absorption Spectra of Sol-gel and Co-precipitation method.

From the result, the optical band gap value is different in different solvents. Using the solvent methanol could be assigned to the difference in a lattice defects and quantum confinement due to decrease in crystallite size i.e. the optical band gap of the nanoparticles was the particle size dependent. As the particle sizes of synthesized samples were larger than the exciton Bohr radius of  $\text{SnO}_2$  (2.7 nm), considered under the weak confinement regime (Li *et al.*, 2011). Even in weak confinement regime, the particle size is very important to tune the optical band gap. From the result, the optical band gap of nanoparticle synthesized by sol-gel method and Co-precipitation method will increase with the decrease in particle size (Dijken *et al.*, 2000). Thus, the use of different solvent during synthesis affects the optical properties of  $\text{SnO}_2$  nanoparticles.

### CONCLUSION

The significance of preparation methods, sol-gel and chemical-precipitation, it was established that the structural, surface morphology and optical properties of  $\text{SnO}_2$  NPs considerably depend on the solvent in employment during synthesis. The particle size of  $\text{SnO}_2$  NPs synthesized by the sol-gel and the chemical-precipitation methods using different solvents was 16.71, 5.43, 10.09 nm and 18.9, 9.9, 11.7 nm respectively. The X-ray diffraction result established the rutile phase, and the nanoscale character of the  $\text{SnO}_2$ . In sol-gel method the band gap is established to be 3.67 eV, 3.63 eV, 3.57 eV equivalent to nanoparticles synthesized by different solvent (water, methanol, ethanol), respectively. In the Co-precipitation method, the band gap is established to be 3.62 eV, 3.59 eV, 3.52 eV synthesized by different solvent (water, methanol, ethanol), respectively.

### Competing Interests

The authors declare that they have no competing interests.

### Acknowledgements

We acknowledged UGC-BSR meritorious fellowship for providing funding support. The author would like to thank DST-FIST (2009) for the PXDR facility and DST-PURSE, for SEM facility.

### References

- Adnan, R. Razana, N.A. Rahman, I.A. and Farrukh, M.A. (2010). Synthesis and Characterization of High Surface Area Tin Oxide Nanoparticles via the Sol-Gel Method as a Catalyst for the Hydrogenation of Styrene. *Journal of the Chinese Chemical Society* 57, 222-229.
- Alivisatos, A.P. (1996). Perspectives on the Physical Chemistry of Semiconductor Nanocrystals. *J. Phys. Chem* 100: 13226-13239.
- Allaedini, G. Tasirin, S.M. Talib, M.Z.M. Aminayi, P. Puspasari, I. (2015). Comparative study on the microstructure and photoluminescence properties of  $\text{SnO}_2$  nano particles prepared by different methods. *Applied Mechanics and Materials* (719-720): 132-136.
- Burda, C. Chen, X. Narayanan, R. and El-Sayed, M.A. (2005). Chemistry and Properties of Nanocrystals of Different Shapes. *Chem. Rev* 105(4): 1025-1102.
- Das, S. and Jayaraman, V. (2014).  $\text{SnO}_2$ : A comprehensive review on structures and gas sensors. *Progress in Materials Science* 66: 112-255.
- Deng, D. and Lee, J.Y. (2008). Hollow Core-Shell Mesospheres of Crystalline  $\text{SnO}_2$  Nanoparticle Aggregates for High Capacity  $\text{Li}^+$  Ion Storage. *Chem. Mater* 20: 1841-1846.
- Dijken, A.V. Mulenkamp, E.A. Vanmaekelbergh, D. and Meijerink, A. (2000). Identification of the transition responsible for the visible emission in  $\text{ZnO}$  using quantum size effects. *J. Lumin* 90:123.
- Drevillon, B. Kumar, S. Cabarrocas, P.R.I. Siefert, JM. (1989). *In situ* investigation of the optoelectronic properties of transparent conducting oxide/amorphous silicon interfaces. *Applied physics letters* 54(21): 2088-2090.
- Gautam, S. Thakur, A. Vij, A. Suk, J. Lee, I.J. Park, Y.J. Shin, T.J. Kim, M.G. Shin, H.J. Lee, J.M. Chen, J.M. Song, J. Chae, K.H. (2013). X-ray spectroscopy study of  $\text{Zn}_x\text{Sn}_{1-x}\text{O}_2$  nanorods synthesized by hydrothermal technique. *Thin Solid Films* 546: 250-254.
- Guan, M. Zhao, X. Duan, L. Cao, M. Guo, W. Liu, J. and Zhang, W. (2013). Controlled synthesis of  $\text{SnO}_2$  nanostructures with different morphologies and the influence on photocatalysis properties. *Journal of Applied Physics* 114, 114302.
- Henglein, A. (1989). Small-Particle Research: Physicochemical Properties of Extremely Small Colloidal Metal and Semiconductor Particles. *Chem Rev* 89, 1861-1873.
- Hieu, N.V. Van, P.T.H. Nhan, L.T. Duy, N.V. and Hoa, N.D. (2012). Giant enhancement of  $\text{H}_2\text{S}$  gas response by decorating n-type  $\text{SnO}_2$  nanowires with p-type  $\text{NiO}$  nanoparticles. *Applied Physics Letters* 101: 253106.
- Hu, Z. Oskam, G. and Peter, C. (2003). Seaton, Influence of solvent on the growth of  $\text{ZnO}$  nanoparticles. *Journal of Colloid and Interface Science* 263: 454-460.
- Huang, C. Tang, Z. and Zhang, Z. (2001). Differences between Zirconium Hydroxide ( $\text{Zr(OH)}_4\text{ZnH}_2\text{O}$ ) and Hydrous Zirconia ( $\text{ZrO}_2\text{ZnH}_2\text{O}$ ). *J. Am. Ceram. Soc* 84(7):1637-38.
- Jiang, L. Sun, G. Zhou, Z. Sun, S. Wang, Q. Yan, S. Li, H. Tian, J. Guo, J. Zhou, B. and Xin, Q. (2005). Size-

- Controllable Synthesis of Monodispersed SnO<sub>2</sub> Nanoparticles and Application in Electrocatalysts. *J. Phys. Chem. B* 109(18): 8774-8778.
16. Kennedy, M.K. Kruis, F.E. and Fissan, H. Mehta, B.R. Stappert, S. and Dumpich, G. (2003). Tailored nanoparticle films from monosized tin oxide nanocrystals: Particle synthesis, film formation, and size-dependent gas-sensing properties, *Journal of Applied Physics* 93: 551.
17. Kumar, V. Singh, K. Singh, K. Kumari, S. Kumar, A. and Thakur, A. (2016). Effect of solvent on the synthesis of SnO<sub>2</sub> nanoparticles, AIP Conference Proceedings 1728: 020532.
18. Leite, E.R. Weber, I.T. Longo, E. and Varela, J.A. (2000). A New Method to Control Particle Size and Particle Size Distribution of SnO<sub>2</sub> Nanoparticles for Gas Sensor Applications. *Adv. Mater* 12(13): 965-968.
19. Li, J. Zhao, Y. Wang, N. and Guan, L. (2011). A high-performance carrier for SnO<sub>2</sub> nanoparticles used in lithium ion battery. *Chem. Commun.* 47, 5238-5240.
20. Minami, T. (2000). New n-Type Transparent Conducting Oxides, *MRS Bulletin* 25: 38-44.
21. Niederberger, M. (2007). Nonaqueous Sol-Gel Routes to Metal Oxide Nanoparticles. *Acc. Chem. Res* 40(9): 793-800.
22. Nomura, K. Okabayashi, J. Okamura, K. and Yamada, Y. (2011). Magnetic properties of Fe and Co codoped SnO<sub>2</sub> prepared by sol-gel method, *Journal of Applied Physics* 110: 083901.
23. Park, H. Lee, J. Kim, H. Kim, D. Raja, J. and Yi, J. (2013). Influence of SnO<sub>2</sub>: F/ZnO:Al bi-layer as a front electrode on the properties of p-i-n amorphous silicon based thin film solar cells. *Applied Physics Letters* 102, 191602.
24. Peaker, A.R. and Horsley, B. (1971). Transparent conducting films of Antimony doped tin oxide on glass. *Rev. Sci. Instrum* 42: 1825-1827.
25. Ungula, J. and Dejene, B.F. (2015). Effect of solvent medium on the structural, morphological and optical properties of ZnO nanoparticles synthesized by sol-gel method. *Physica B: Physics of Condensed Matter*, <http://dx.doi.org/10.1016/j.physb.2015.10.007>
26. Vij, A. Gautam, S. Won, S.O. Thakur, A. Lee, I.J. Chae, K.H. (2012). X-ray photoelectron spectroscopy of Zn0.98Cu0.02O thin film grown on ZnO seed layer by RF sputtering. *Materials Letter* 88:51-53.
27. Wang, B. Wang, Z. Cui, Y. Yang, Y. Wang, Z. and Qian, G. (2015). Electrochemical properties of SnO<sub>2</sub> nanoparticles immobilized within a metal-organic framework as an anode material for lithium-ion batteries. *RSC Advances* 5: 84662-84665.
28. Young, D.L. Moutinho, H. Yan, Y. and Coutts, T.J. (2002). Growth and characterization of radio frequency magnetron sputter-deposited zinc stannate, Zn<sub>2</sub>SnO<sub>4</sub>, thin films. *Journal of Applied Physics* 92(1): 310-319.
29. Zhang, J.B. Li, X.N. Bai, S.L. Luo, R.X. Chen, A.F. Lin, Y. (2012). High-yield synthesis of SnO<sub>2</sub> nanobelts by water-assisted chemical vapor deposition for sensor applications. *Materials Research Bulletin* 47: 3277-3282.
30. Zhu, J. Tay, B.Y. and Ma, J. (2006). Synthesis of mesoporous tin oxide on neutral surfactant templates. *Materials Letters* 60(8): 1003-1010.

**How to cite this article:**

Backialakshmi P and Gopinathan C.2017, Influence of Solvent on Structural, Morphological And Optical Properties of SnO<sub>2</sub> Nanoparticles Prepared by Different Methods. *Int J Recent Sci Res.* 8(9), pp. 19800-19804.  
DOI: <http://dx.doi.org/10.24327/ijrsr.2017.0809.0761>

\*\*\*\*\*